Photosynthetic productivity and its efficiencies in ISIMIP2a biome models: benchmarking for impact assessment studies

2017 Environ. Res. Lett. 12 085001

(http://iopscience.iop.org/1748-9326/12/8/085001)

Environmental Research Letters

LETTER

Photosynthetic productivity and its efficiencies in ISIMIP2a biome models: benchmarking for impact assessment studies

Akihiko Ito[1,2,14], Kazuya Nishina[1], Christopher P O Reyer[3], Louis François[4], Alexandra-Jane Henrot[4], Guy Munhoven[4], Ingrid Jacquemin[4], Hanqin Tian[5], Jia Yang[5], Shufen Pan[5], Catherine Morfopoulos[6], Richard Betts[6,7], Thomas Hickler[8,9], Jörg Steinkamp[8], Sebastian Ostberg[3,10], Sibyll Schaphoff[3], Philippe Ciais[11], Jinfeng Chang[11], Rashid Rafique[12], Ning Zeng[13] and Fang Zhao[3]

[1] National Institute for Environmental Studies, 16-2 Onogawa, Tsukuba 3058506, Japan
[2] Japan Agency for Marine-Earth Science and Technology, Yokohama 2360001, Japan
[3] Potsdam Institute for Climate Impact Research, Potsdam D-14412, Germany
[4] Unité de Modélisation du Climat et des Cycles Biogéochimiques (UMCCB), Université de Liège, Liège B-4000, Belgium
[5] International Center for Climate and Global Change Research, School of Forestry and Wildlife Sciences, Auburn University, Auburn, AL 36849, United States of America
[6] University of Exeter, Exeter EX4 4QF, United Kingdom
[7] Hadley Centre, MetOffice, Exeter EX1 3PB, United Kingdom
[8] Senckenberg Biodiversity and Climate Research Centre, Frankfurt am Main 60325, Germany
[9] Goethe University, Frankfurt am Main 60325, Germany
[10] Humboldt-Universität zu Berlin, Berlin 10099, Germany
[11] Laboratoire des Sciences du Climat et de l'Environnement, Gif-sur-Yvette 91191, France
[12] Joint Global Change Research Institute, Pacific Northwest National Laboratory, College Park, MD 20740, United States of America
[13] University of Maryland, College Park, MD 20742, United States of America
[14] Author to whom any correspondence should be addressed.

E-mail: itoh@nies.go.jp

Keywords: carbon cycle, gross primary production, ISIMIP2a, modeling, uncertainty, vegetation

Supplementary material for this article is available online

OPEN ACCESS

RECEIVED
14 January 2017

REVISED
29 May 2017

ACCEPTED FOR PUBLICATION
19 June 2017

PUBLISHED
25 July 2017

Abstract

Simulating vegetation photosynthetic productivity (or gross primary production, GPP) is a critical feature of the biome models used for impact assessments of climate change. We conducted a benchmarking of global GPP simulated by eight biome models participating in the second phase of the Inter-Sectoral Impact Model Intercomparison Project (ISIMIP2a) with four meteorological forcing datasets (30 simulations), using independent GPP estimates and recent satellite data of solar-induced chlorophyll fluorescence as a proxy of GPP. The simulated global terrestrial GPP ranged from 98 to 141 Pg C yr^{-1} (1981–2000 mean); considerable inter-model and inter-data differences were found. Major features of spatial distribution and seasonal change of GPP were captured by each model, showing good agreement with the benchmarking data. All simulations showed incremental trends of annual GPP, seasonal-cycle amplitude, radiation-use efficiency, and water-use efficiency, mainly caused by the CO_2 fertilization effect. The incremental slopes were higher than those obtained by remote sensing studies, but comparable with those by recent atmospheric observation. Apparent differences were found in the relationship between GPP and incoming solar radiation, for which forcing data differed considerably. The simulated GPP trends co-varied with a vegetation structural parameter, leaf area index, at model-dependent strengths, implying the importance of constraining canopy properties. In terms of extreme events, GPP anomalies associated with a historical El Niño event and large volcanic eruption were not consistently simulated in the model experiments due to deficiencies in both forcing data and parameterized environmental responsiveness. Although the benchmarking demonstrated the overall advancement of contemporary biome models, further refinements are required, for example, for solar radiation data and vegetation canopy schemes.

1. Introduction

Photosynthetic productivity is a fundamental function of the terrestrial biosphere and is related to various ecosystem properties and services (Whittaker and Likens 1973). Gross primary production (GPP) is one of the largest carbon flows in the global carbon cycle and responds to changes in various environmental conditions such as light, temperature, humidity, nutrient, and ambient carbon dioxide (CO_2) conditions. Any changes in GPP can affect atmospheric CO_2 and thus the climate–carbon cycle feedback (e.g. Cox *et al* 2000).

Quantifying GPP under a changing environment is a challenging task, however, not only for modeling but also for observation. This issue is a serious limitation of present carbon cycle models, which have been used for future projection and impact assessments (Friedlingstein *et al* 2006, Arora *et al* 2013). Even with updated micrometeorological techniques such as the eddy-covariance method (Baldocchi *et al* 2001), GPP cannot be directly measured and must be estimated from net CO_2 flux using appropriate separation algorithms (Reichstein *et al* 2005). Beer *et al* (2010) scaled up field-based GPP data using a statistical model approach to produce a global map of GPP, although the assumptions used in the estimation can introduce certain biases (Wehr *et al* 2016). GPP has also been estimated by satellite remote sensing based on the relationship between canopy-absorbed solar radiation and GPP, using the light-use efficiency approach (e.g. Zhao *et al* 2005). Recent global GPP estimation studies have provided useful data to investigate spatial and temporal patterns of the terrestrial carbon budget (Ryu *et al* 2011, Koffi *et al* 2013, Yan *et al* 2015, Yebra *et al* 2015, Zhang *et al* 2016a). Nevertheless, consistent global GPP values have not been attained (Baldocchi *et al* 2015). For example, an isotopic study by Welp *et al* (2011) implied that global GPP is much higher than the values obtained by flux and satellite studies. In contrast, an analysis by Ma *et al* (2015) implied that previous studies have overestimated global forest GPP because of an incorrect assumption of forest coverage change. Terrestrial ecosystem models have been successfully adopted in carbon cycle studies, but large uncertainties remain in their estimates (Anav *et al* 2015, Schwalm *et al* 2015). They adopt different leaf- and canopy-photosynthetic schemes, which respond diversely to environmental variability, and they use different forcing data, leading to serious uncertainties and preventing reliable risk assessments.

In this study, we examined global terrestrial GPP estimated by eight biome models of the Inter-Sectoral Impact Model Intercomparison Project (ISIMIP). The chief aim of the second phase (ISIMIP2a) is the benchmarking of impact models focusing on inter annual variability (Rosenzweig *et al* 2017, Frieler *et al* in prep). To clarify the reliability and limitations of existing models, benchmarking (or validation) has become increasingly important in all research areas of modeling (Luo *et al* 2012, Kelley *et al* 2013). Indeed, Chang *et al* (2017) conducted a benchmarking of ISIMIP2a biome models with respect to the net ecosystem carbon budget, focusing on the impact of El Niño and Southern Oscillation (ENSO) events. In this paper, we examine consistency in major aspects of (mainly global annual ones for brevity) of GPP estimated using different biome models and forcing data thorough comparisons with independent estimates and observational data.

2. Methods

2.1. Biome models and simulations

In ISIMIP2a, to examine model responsiveness and limitations in forcing data, we used four meteorological forcing datasets for the historical period (Sheffield *et al* 2006, Weedon *et al* 2014): Global Soil Wetness Project 3 (GSWP3, 1901–2010), Water and Global Change (WATCH, 1901–2001), WATCH Forcing Data with ERA-Interim (WFDEI, 1901–2010), and Princeton's Global Meteorological Forcing Dataset (Princeton, 1901–2012). These datasets provide daily solar radiation, temperature, precipitation, humidity, and wind conditions at a spatial resolution of $0.5° \times 0.5°$ in latitude and longitude. They were produced from different reanalysis data and by different downscaling methods to cover the range of uncertainty in forcing data. De-trended 30-yr data were also provided for each dataset to conduct spin-up runs under a stationary condition. Historical changes in atmospheric CO_2 concentration were prescribed by combining data from Meinshausen *et al* (2011) through 2005 and Dlugokencky and Tans (2014) from 2006 to 2013. See the ISIMIP web page (www.isimip.org/) for the detailed simulation protocol and model description.

In the biome sector, eight models provided simulation output (table 1). These models differ in structure of the biogeochemical scheme and parameterization of vegetation dynamics, and thus in their responsiveness to environmental change. As revealed in the first phase of ISIMIP, the biome models produce substantially different projections of productivity, biomass, and soil carbon pool (Friend *et al* 2014, Nishina *et al* 2015). In terms of GPP calculation, the models differ in parameterizations of canopy radiation transfer, leaf phenology, and physiological limitation on photosynthetic capacity. Moreover, the model simulations differ in consideration of land-use change, with several models assuming fixed land use throughout the simulation period.

2.2. Benchmarking datasets

We used two global GPP data-driven products, which are independent of the ISIMIP simulations, for benchmarking of annual and monthly GPP. First, we adopted the satellite-derived GPP product based on Moderate

Table 1. Summary of biome models and simulations.

Biome models	GPP-estimation scheme	GSWP3	Princeton	WATCH	WFDEI	Reference
CARAIB (Carbon Assimilation in the Biosphere)	3-component canopy scheme with Farquhar biochemical photosynthesis	X	X	X	X	Dury *et al* 2010
DLEM (Dynamic Land Ecosystem Model)	2-component canopy scheme with Farquhar and Collatz biochemical photosynthesis	X	X	X	X	Tian *et al* 2011
JULES (Joint UK Land Environment Simulator, University of Exeter)	2-component canopy scheme with Farquhar and Collatz biochemical photosynthesis	X	X	X	–	Clark *et al* 2011
LPJ-GUESS (Lund Potsdam Jena General Ecosystem Simulator)	Canopy scheme with Haxeltine-Prentice photosynthesis	X	X	X	X	Smith *et al* 2001
LPJmL (Lund Potsdam Jena model with managed Land)	Canopy scheme with Haxeltine-Prentice photosynthesis	X	X	X	X	Bondeau *et al* 2007
ORCHIDEE (Organizing Carbon and Hydrology in Dynamic EcosystEms)	Canopy scheme with Farquhar photosynthesis with Ball stomata model	X	X	X	X	Krinner *et al* 2005
VEGAS (Vegetation Global Atmosphere Soil)	Canopy scheme with light-use efficiency approach	X	–	X	X	Zeng *et al* 2005
VISIT (Vegetation Integrative Simulator for Trace gases)	1-layer canopy scheme scaled-up from Leuning stomatal leaf gas exchange	X	X	X	X	Ito and Inatomi 2012

Resolution Imaging Spectroradiometer (MODIS; Zhao *et al* 2005) fAPAR and a light-use efficiency model from 2000 to 2012. The original data, which were in GeoTIFF format with a 5′-mesh grid, were averaged and converted into 0.5°-mesh. Second, we adopted up-scaled flux measurement data (Beer *et al* 2010) from 1982 to 2011; the original spatial resolution of the data was 0.5°. The data were produced using site-based flux measurement data, climate data, SeaWiFS vegetation index, and a regression-model ensemble algorithm (Jung *et al* 2009). These data were used for benchmarking of GPP by grid-based linear regression. Note that the CARBONES GPP dataset (Kuppel *et al* 2014), although adopted by other studies (e.g. Anav *et al* 2015), was not used in this study, because the dataset is a hybrid of observational data and the ORCHIDEE simulation.

Simulated GPP values were also correlated with solar-induced fluorescence (SIF; mW m^{-2} nm^{-1} sr^{-1}) data at the far-red peak (wavelength 737 nm) measured by the Global Ozone Monitoring Instrument 2 (GOME-2; Joiner *et al* 2013). SIF is expected to be closely correlated with biophysical and biochemical properties and processes of photosynthesis (e.g. quantum yield; Genty *et al* 1989). In particular, SIF from satellites tends to capture vegetation activity under clear sky conditions, in which photosynthesis and fluorescence respond in a similar manner (Porcar-Castell *et al* 2014). Therefore, observed SIF data have been used for model benchmarking as a proxy of GPP (Guanter *et al* 2014, Zhang *et al* 2016b). However, SIF is not completely linked with photosynthetic biophysical processes, and the data contain intrinsic noises and biases due to low signal levels. The GOME-2 SIF data are, even at a monthly basis, a bit noisy for grid-based comparison at the original 1°-mesh resolution, so they were used after aggregation into a 5°-mesh during the period from 2007 to 2010.

2.3. Analyses and metrics

We obtained data of 30 simulations (table 1) and structured the comparisons in terms of forcing data and biome models. Basic metrics such as mean, standard deviation, and coefficient of variation (standard deviation divided by the mean) were examined first. Metrics specific to biospheric studies such as long-term mean, seasonal change, interannual change, and linear trend of GPP were also examined. To separate the variabilities caused by forcing data and biome models, two-way analysis of variance (ANOVA) was conducted (R 3.4.0; R Core Team 2017) for the 30 global annual mean GPP estimates in 1981–2000. For grid-based benchmarking, the mean annual GPP in 2001–2010 for each grid was correlated with those estimated by using MODIS and flux up-scaling data. We also performed correlation analysis on the 5°-averaged GPP values and GOME-2 SIF data to assess their relationship.

Several metrics related to GPP properties were examined. Seasonal-cycle amplitude (SCA) of GPP, which reflects vegetation activity and affects atmospheric CO_2 (Graven *et al* 2013, Wenzel *et al* 2016), was defined as the difference between the maximum and minimum monthly values for each year. Resource-use efficiencies of GPP are expected to provide insights into underlying mechanisms and limiting factors of photosynthetic production. Based on the incoming solar radiation data and simulated GPP and evapotranspiration, we calculated radiation-use efficiency (RUE) and water-use efficiency (WUE) as follows:

$$\mathrm{RUE} = \mathrm{GPP}/\mathrm{DSR} \quad (1)$$

and

$$\mathrm{WUE} = \mathrm{GPP}/\mathrm{TR} \quad (2)$$

Table 2. Summary of estimated GPP values and their trends.

Biome model	GPP, 1981–2000 (Pg C yr^{-1})					Mean trend, 1981–2000 (% yr^{-1})			
Forcing data	GSWP3	Princeton	WATCH	WFDEI	SD	GPP	WUE	RUE	SCA
CARAIB	126.5	141.2	130.6	133.1	6.2	0.49	0.28	0.35	0.32
DLEM	108.1	108.8	106.2	105.9	1.4	0.32	0.23	0.30	0.32
JULES	98.4	99.9	101.9		1.8	0.30	0.22	0.27	0.22
LPJ-GUESS	117.5	119.3	111.8	117.0	3.2	0.39	0.29	0.36	0.17
LPJmL	126.7	126.8	120.6	125.0	2.9	0.25	0.16	0.23	0.03
ORCHIDEE	104.5	116.6	107.3	106.9	5.3	0.26	0.23	0.24	0.26
VEGAS	106.3		108.2	111.0	2.3	0.19	0.06	0.20	0.13
VISIT	133.4	121.1	113.4	115.6	8.9	0.28	0.15	0.26	0.16
Mean	115.2	119.1	112.5	116.3		0.31	0.20	0.28	0.20
SD	12.7	13.1	9.2	9.9		0.09	0.08	0.06	0.10

Table 3. Summary of model intercomparison projects of biome models.

Project name	Period	Forcing meteorological data	Description and experiments	GPP range (Pg C yr^{-1})
CMIP5 (Anav *et al* 2015)	1850–2005	Climate models driven by historical GHG concentration	Earth-system model experiments including biogeochemical feedbacks	130–169
MsTMIP (Schwalm *et al* 2015)	1901–2010	CRU-NCEP	Factor-out of climate, land-use, atmospheric CO_2, and N deposition	99–187
TRENDY (Sitch *et al* 2015)	1901–2009	CRU-NCEP	Factor-out of climate, land-use, and atmospheric CO_2	(51.5–75.5 for net primary production)
ISI-MIP (this study)	1971–2012	GSWP3, Princeton, WATCH, WFDEI	Comparison of different forcing data for benchmarking	98.4–141.2

where DSR is downward short wave radiation at the land surface and TR is vegetation transpiration. In general, photosynthetically active radiation (PAR) accounts for about 48% of DSR (McCree 1972), and RUE as defined by equation (1) may be easily converted into a PAR-based value. For the DLEM, JULES, and VEGAS models, WUE was calculated using total evapotranspiration rates, because TR data files were not supplied for these models. Therefore, in this study, inter-model comparisons were made only for relative change from the 1996–2000 annual average. Note also that RUE could be defined using solar radiation absorbed by the canopy (e.g. Ruimy *et al* 1999), which is inferred from leaf area index and the canopy attenuation coefficient (typically 0.5) of Lambert-Beer's law. However, because a few models do not supply leaf area index data, we used equation (1), which is applicable to all model runs.

3. Results and discussion

3.1. Global terrestrial GPP by biome model

Global terrestrial GPP simulated by the biome models using the four forcing datasets during the common overlapping period of 1981–2000 was 115.7 ± 11.0 Pg C yr^{-1} (mean ± standard deviation of all simulations), ranging from 98.4 to 141.2 Pg C yr^{-1} (table 2). Although this may seem to be a broad range, most values fell within the range of previously reported values (table 3). Most of the simulated GPP values were not very different from those of MODIS (112 Pg C yr^{-1}, 2000–2012) and flux up-scaled (132 Pg C yr^{-1}, 1982–2011) estimates.

Table 4. Summary of ANOVA for mean global GPP.

Factor	Degrees of freedom	Sum of square	Mean square	*F* value	*p* value
Forcing data	3	167.1	55.7	2.698	0.0748
Biome model	7	2947.2	421	20.97	0.01
Residuals	19	392.2	20.6		

As shown by the ANOVA result (table 4), the variability in the estimated global GPP was primarily attributable to inter-model variability (84% of total); inter-data variability and residual (interaction term) accounted for 4.8% and 11%, respectively. Apparent inter-model differences were found, ranging from 100.1 ± 1.8 Pg C yr^{-1} for JULES to 133.1 ± 6.2 Pg C yr^{-1} for CARAIB. In contrast, model-ensemble GPP was not significantly different among the four forcing datasets, ranging from 112.5 ± 9.2 Pg C yr^{-1} for WATCH to 116.3 ± 9.9 Pg C yr^{-1} for WFDEI (table 2). In terms

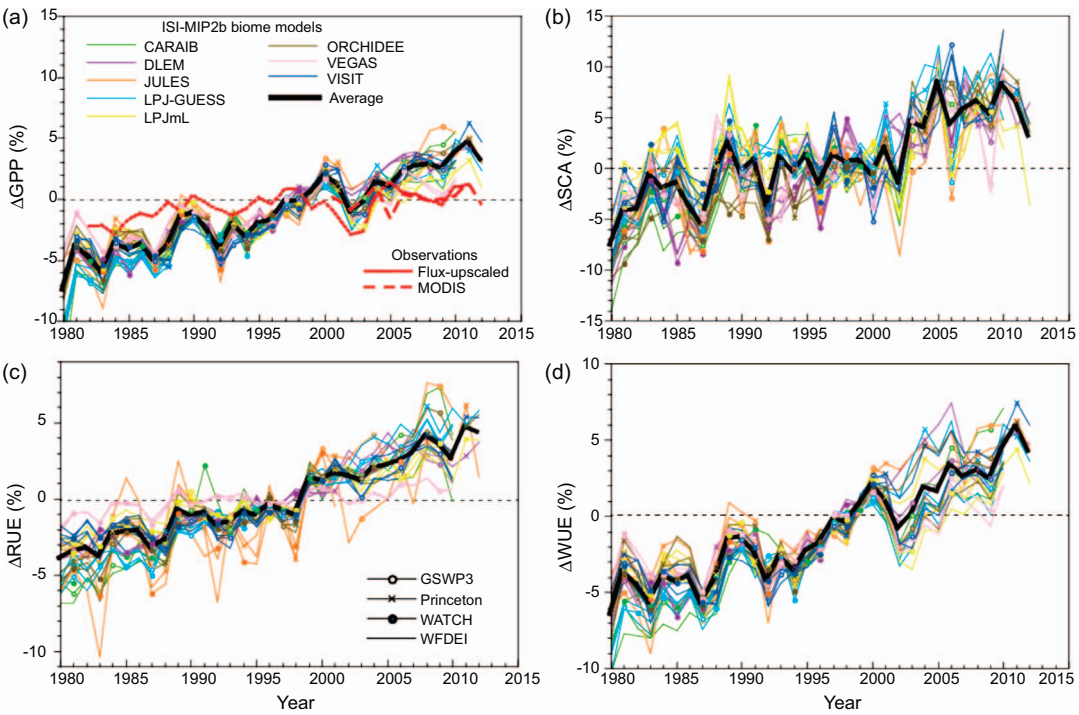

Figure 1. Annual time-series of terrestrial ecosystem functions and efficiencies simulated by the eight biome models with four forcing datasets: (*a*) gross primary production (GPP), (*b*) seasonal-cycle amplitude (SCA), (*c*) radiation-use efficiency (RUE), and (*d*) water-use efficiency (WUE). For each dataset, anomalies (denoted by Δ) from the 1996–2000 mean are shown. For GPP in (*a*), data from MODIS (anomalies from the 2000–2012 mean) and flux up-scaled GPP (1982–2011) are included.

of differences among the forcing datasets, DLEM showed the smallest variability (2.9 Pg C yr^{-1}) and VISIT the largest variability (20.0 Pg C yr^{-1}) between the maximum and minimum values. Few common patterns were found in the dependence on forcing data among the biome models. Four biome models (DLEM, LPJ-GUESS, LPJmL, and ORCHIDEE) simulated the highest GPP when using the Princeton forcing data, and four models (CARAIB, JULES, ORCHIDEE, and VEGAS) simulated the lowest GPP when using the GSWP3 forcing data. For three datasets, CARAIB estimated the highest GPP among the models. Different, inconsistent patterns were found in other cases.

3.2. Trends in GPP

The simulated global terrestrial GPP showed similar interannual variability, irrespective of biome model and forcing data. The average slope of the linear trend was estimated as $0.30 \pm 0.07\%$ yr^{-1} or 0.35 ± 0.09 Pg C yr^{-2}, and differed among simulations: from the shallowest slope in VEGAS driven by GSWP3 data (0.19% yr^{-1}) to the steepest slope in LPJ-GUESS driven by WATCH data (0.41% yr^{-1}). These GPP slopes were steeper than those of the flux up-scaling (0.14% yr^{-1}, 1982–2000; 0.08% yr^{-1}, 1982–2011) and satellite observation (0.035% yr^{-1}, 2000–2012). Kolby Smith *et al* (2015) found similarly higher incremental trends of terrestrial net primary productivity estimated by the CMIP5 models: $7.6 \pm 1.67\%$ in 1982–2011 (i.e. $0.25 \pm 0.06\%$ yr^{-1}). They implied that the present models overestimate the vegetation response to elevated CO_2 due to insufficiencies in model parameterization such as nitrogen limitation (Zaehle *et al* 2014, Schimel *et al* 2015). In contrast, a recent study (Campbell *et al* 2017) of long-term atmospheric observation of carbonyl sulfide showed that terrestrial GPP has increased at a higher rate than previously thought before: $31 \pm 5\%$ in the 20th century (assuming linearity, $0.31 \pm 0.05\%$ yr^{-1}). While their results show higher incremental trends in the late 20th century, the mean incremental trend by ISIMIP2a models is comparable with the atmospheric observation-based estimate. Because inconsistency remains in observational evidence, model studies as conducted here are important to perform sensitivity analyses and to resolve underlying mechanisms.

The SCA of GPP also showed incremental trends (figure 1(*b*)), on average $0.20 \pm 0.11\%$ yr^{-1}, implying that temperate and boreal vegetation contributed at least partly to the GPP increase and that vegetation phenology (e.g. growing season length) could have been affected in these regions. The estimated SCA incremental trends spans from −0.018% yr^{-1} in LPJmL driven by Princeton to 0.42% yr^{-1} in CARAIB driven by WFDEI (see table 2 for data-ensemble results). Such incremental trends and inter-model variability have also been found in previous studies (Zhao and Zeng 2014, Ito *et al* 2016) and are consistent with satellite-observed greening of northern vegetation (Zhu *et al* 2016). Among the GPP-related properties, the SCA trends showed the largest variability among the simulations. The average RUE

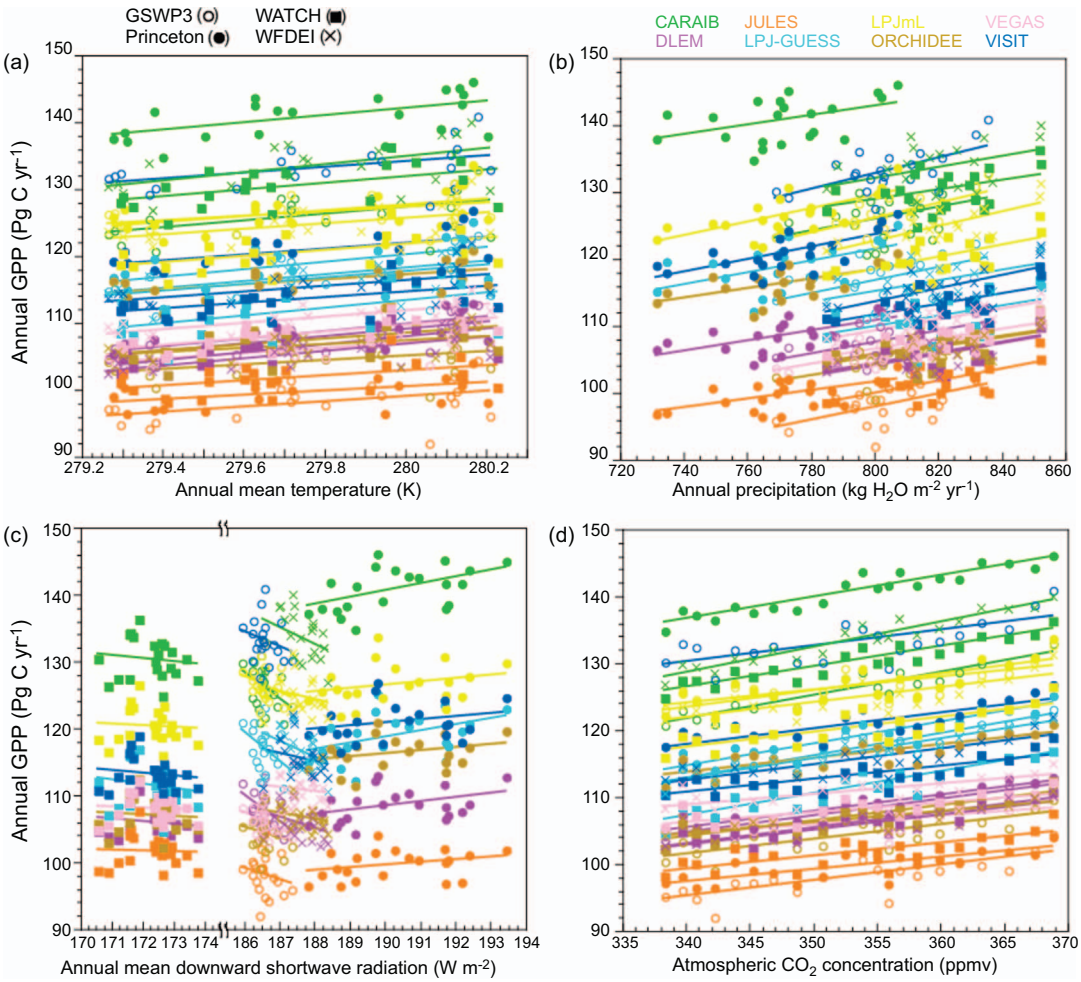

Figure 2. Relationships between terrestrial gross primary production (GPP) simulated by eight biome models driven by four forcing datasets and (*a*) global mean annual temperature, (*b*) global annual precipitation, (*c*) global downward shortwave radiation (no data between 174 and 186 W m^{-2}), and (*d*) atmospheric CO_2 concentration.

of GPP was calculated as 0.156 ± 0.015 g C MJ^{-1} in the simulations, and its mean trend was calculated as $0.28 \pm 0.06\%$ yr^{-1} (figure 1(*c*)). None of the forcing data showed a clear decadal trend such as global dimming and brightening (Wild 2012), so the incremental trend in RUE was primarily caused by the GPP increase. Simulated global transpiration (data not shown) indicated moderate incremental trends: $0.088 \pm 0.037\%$ yr^{-1}. This transpiration increment was mainly related to vegetation activity (e.g. leaf area expansion), while land precipitation did not show a clear decadal trend. Consequently, estimated WUE showed clear incremental trends (figure 1(*d*)): $0.20 \pm 0.076\%$ yr^{-1}. Among the biome models, the WUE trend spanned from 0.06% yr^{-1} for VEGAS to 0.287% yr^{-1} for LPJ-GUESS. The incremental trend of WUE was largely attributable to the increase of GPP. Both experimental and theoretical studies suggest that water loss by transpiration does not increase quantitatively in parallel with photosynthetic carbon assimilation due to stomatal regulation of gas exchange (Medlyn *et al* 2001, Bonan *et al* 2014). Also, observational and modeling studies indicated that biospheric WUE has increased, mainly as a result of elevated CO_2 (Keenan *et al* 2013, Xue *et al* 2015), which enhances photosynthesis but restricts transpiration by stomatal closure.

3.3. Meteorological variability and GPP

To clarify the characteristics of environmental responsiveness, which should account for inter-model variability, the estimated GPP values were correlated with temperature, precipitation, solar radiation, and CO_2 conditions for 1981–2000. For temperature, the inter annual variability was comparable among the four forcing datasets (figure 2(*a*)). The estimated GPP responded similarly to temperature variability irrespective of forcing data and biome models, with values ranging from 3.1 Pg C yr^{-1} K^{-1} (ORCHIDEE driven by WFDEI) to 6.1 Pg C yr^{-1} K^{-1} (DLEM driven by WATCH). For precipitation, a moderate difference was found among the forcing data, from 772 kg H_2O m^{-2} yr^{-1}(Princeton) to 821 kg H_2O m^{-2} yr^{-1} (WATCH; figure 2(*b*)). The biome models showed comparable positive responsiveness to precipitation, spanning from 0.064 Pg C yr^{-1} (kg H_2O m^{-2} $yr^{-1})^{-1}$ (JULES driven by Princeton) to 0.117 Pg C yr^{-1} (kg H_2O m^{-2} $yr^{-1})^{-1}$ (VISIT driven by GSWP3). For solar

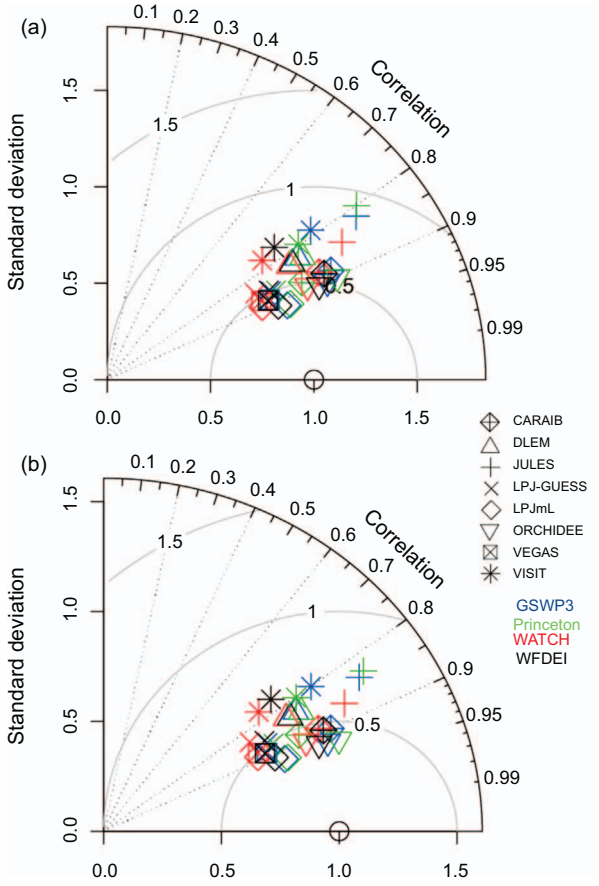

Figure 3. Taylor diagrams of annual gross primary production (GPP) simulated by eight biome models using four meteorological forcing datasets relative to (*a*) MODIS GPP and (*b*) flux up-scaled GPP. The correlation and standard deviation were calculated for the period 2000–2010 for the GSWP3, Princeton, and WFDEI cases. In the WATCH cases, the simulated GPP in 1990–2000 was used due to the limitation of the simulation length.

radiation, a conspicuous difference was found among the forcing data, spanning from 172 W m^{-2}(WATCH) to 190 W m^{-2} (Princeton). These forcing data also differed in decadal trends and interannual variability. For example, only the Princeton data showeda clear incremental trend (+0.14 W m^{-2} yr^{-1}) with large interannual variability, whereas the others showed small negative trends. Remarkably, the biome models responded differently to solar radiation among the forcing data (figure 2(*c*)); the estimated GPP only responded positively to solar radiation in Princeton-driven simulations. The high solar radiation in the Princeton dataset may be associated with the high GPP of five models (CARAIB, DLEM, LPJ-GUESS, LPJmL, and ORCHIDEE; table 2). Because solar radiation is important not only for GPP estimation but also for Earth's energy budget (Kiehl and Trenberth 1997), improvement of the solar radiation dataset is of great significance.

3.4. Benchmarking

The spatial distribution of GPP simulated by different biome models agreed for overall continental-scale patterns (supplementary figures S1 and S2, available at stacks.iop.org/ERL/12/085001/mmedia), such as gradients from high GPP in equatorial rain forests to low GPP at high latitudes and in deserts. However, inter-model differences were evident regionally at sub-continental scales. For example, JULES showed a sharp transition of GPP from tropical forests to surrounding rangelands, whereas LPJ-GUESS and VEGAS showed more gradual transitions. The spatial distribution of the coefficient of variation of simulated GPP values (figure S2(*c*)) showed higher variability in low-GPP areas such as arid regions (e.g. central Eurasia, North Africa, and Australia) and Arctic tundra. Among the models, LPJmL showed the highest coefficients of determination ($R^2 \approx 0.92$) with the reference data (figure 3); others also showed R^2 values of 0.8 or higher. The benchmarking of annual GPP using independent datasets confirmed that the biome models could capture the major global patterns of photosynthetic productivity as obtained by up-scaling and remote sensing approaches. Along with advancements in the flux measurement dataset and machine-learning algorithms, further useful field-based datasets (e.g. Jung *et al* 2017) will become available for model benchmarking.

The relationship between simulated GPP and satellite-observed SIF data (figure 4) seems reasonable, considering the noisiness of the data. In most biome models, simulated GPP was linearly related

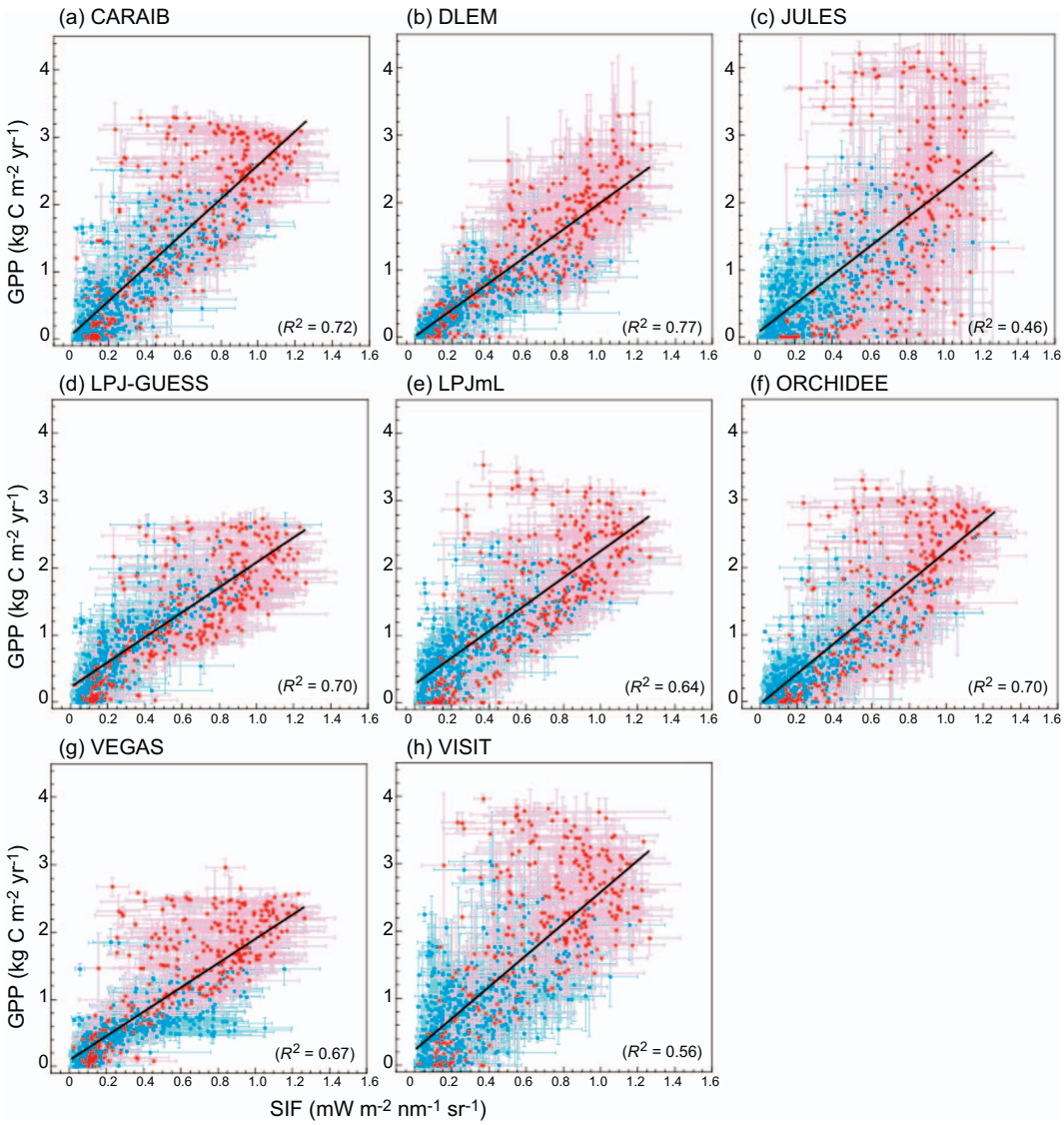

Figure 4. Global relationship between sun-induced chlorophyll fluorescence (SIF) from GOME-2 and gross primary production (GPP) simulated by the eight biome models (*a*–*h*), during the period 2007–2010 using the GSWP3 forcing dataset. Black lines show linear regression (R^2 in parentheses). Both SIF and GPP data were aggregated into 5°-mesh to reduce the influence of observational noise; bars show the standard deviation within the 5°-grids. Red dots show tropical areas (25°N–25°S), and blue dots show temperate and borealareas.

to the corresponding SIF values, and DLEM showed the highest R^2 value for the relationship. Several models (e.g. JULES and VISIT) estimated high GPP in low-SIF areas, resulting in somewhat lower R^2 values. As demonstrated in previous studies (e.g. Anav *et al* 2015, Zhang *et al* 2016b), simulated GPP and SIF data show comparable seasonal cycles in temperate and boreal ecosystems. Because SIF is more intimately coupled with photosynthetic biophysical processes, benchmarking with SIF is expected to provide additional information on vegetation activity. Indeed, Zhang *et al* (2016c) used SIF data to obtain an ensemble GPP by weighting estimates by multiple models. We confirmed that monthly GPP simulated by the biome models shows comparable seasonal change with that in SIF (figure S3). In tropical areas, however, the seasonal signal was very weak, and such correspondence was unclear (figure S3(*c*)), implying that several models have difficulty with the environmental responsiveness of tropical ecosystems. In accordance with its effectiveness as a proxy of photosynthetic activity, more and higher-quality SIF data will soon be provided by satellites, including the Greenhouse gas Observation Satellite (GOSAT; Frankenberg *et al* 2011) of Japan and the Fluorescence Explorer (FLEX) of the European Space Agency. We expect a considerable increase in usage of SIF data by terrestrial vegetation studies in the coming years.

The benchmarking of global terrestrial GPP revealed different characteristics of the participant models. For example, LPJmL and ORCHIDEE captured long-term mean GPP with higher agreement with observational data than the others. DLEM showed better agreement with SIF data and smaller inter-data variability. VEGAS showed slightly lower GPP and smaller incremental trends, whereas

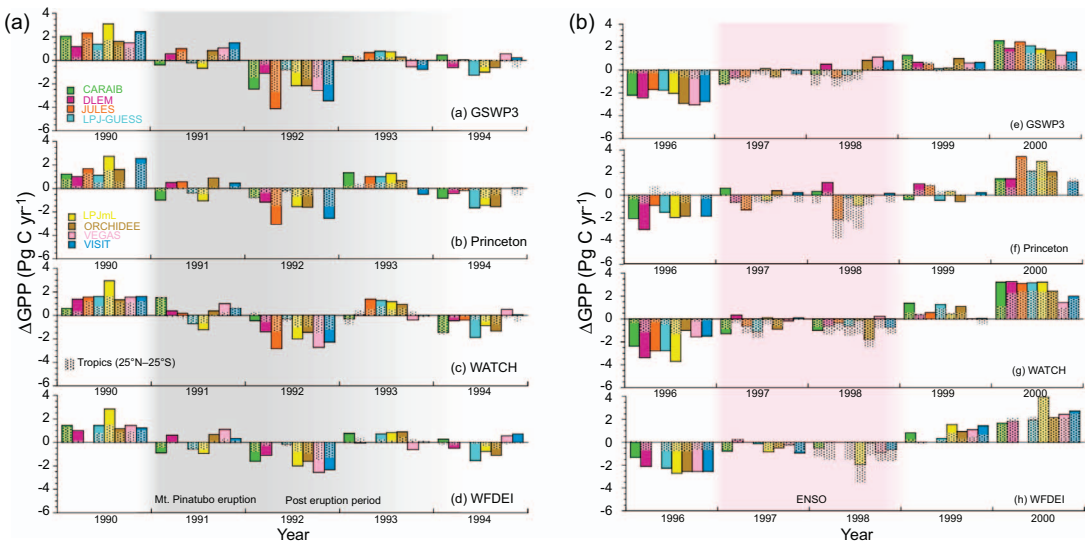

Figure 5. Anomalies of annual gross primary production (GPP) simulated by eight biome models driven by four forcing datasets (*a*) from 1990 to 1994 (before and after the Mt. Pinatubo eruption in June 1991) and (*b*) from 1996 to 2000 (before and after the strong 1997–1998 ENSO event). Hatched areas show the contribution of tropical (25°N–25°S) ecosystems.

CARAIB showed relatively higher GPP and larger trends. LPJ-GUESS captured intermediate mean annual GPP and larger incremental trends. JULES and VISIT showed lower or higher total GPP but captured intermediate incremental trends. Therefore, we should be aware that the current biome models have their own pros and cons, and we need caution in specifying which model works best for a given purpose (e.g. analysis of temporal variability, spatial mapping, and biogeochemical process study). Better understanding of such model characteristics is useful for interpret impact simulation results.

3.5. Impacts of extreme events

In the context of model benchmarking and global change study, extreme events are gathering increasing attentions. Here we focused on two extreme events: the huge eruption of Mt. Pinatubo in 1991 (McCormick *et al* 1995) and the strong ENSO in 1997–1998. Simulated global GPP markedly decreased after the Mt. Pinatubo eruption irrespective of biome model and forcing dataset (figure 5(*a*)). Model-mean GPP anomalies in 1992 differed among the forcing datasets, ranging from $-1.51\,\mathrm{Pg\,C\,yr^{-1}}$ for WFDEI cases to $-2.25\,\mathrm{Pg\,C\,yr^{-1}}$ for GSWP3 cases. In contrast, observational evidence suggests that the terrestrial biosphere could absorb more carbon, which would account for the decline in the atmospheric CO_2 growth rate observed after the eruption (Keeling *et al* 1995). The time-series of solar radiation in the forcing data showed few volcanic signals after the eruption event (data not shown): only the WATCH dataset shows a clear decline in solar radiation by (about $2\,\mathrm{W\,m^{-2}}$) in 1992. Moreover, the forcing datasets did not contain a variable for the diffuse component of solar radiation. Several studies revealed the importance of diffuse radiation for the increased canopy radiation absorption and carbon assimilation (Roderick *et al* 2001, Gu *et al* 2002, Kanniah *et al* 2013), which would explain the low CO_2 growth rate after the huge volcanic eruption. By appropriately including solar radiation factors, several model studies have successfully simulated the change in terrestrial carbon budget after the volcanic eruption (Lucht *et al* 2002, Frölicher *et al* 2013). In the present study and other multi-model studies (e.g. Le Quéré *et al* 2015), however, most biome models were unsuccessful in simulating the anomalous GPP increase after the eruption.

Many studies have assessed the impacts of ENSO events on the terrestrial carbon budget, which affects the atmospheric CO_2 growth rate (e.g. Zeng *et al* 2005, Betts *et al* 2016). The ENSO event in 1997–1998 was the strongest one in the simulation period, and was accompanied by a high atmospheric CO_2 growth rate. In 1998, the warmest year in the 20th century, most models estimated negative GPP anomalies in the tropics (figure 5(*b*)). In the cases of LPJml driven by WFDEI and JULES driven by Princeton, tropical GPP dropped down by as much as $4\,\mathrm{Pg\,C\,yr^{-1}}$ as compared with other years. In contrast, several models responded only moderately to the ENSO event. The warmth in the ENSO period could lead to a longer growing period for temperate and boreal vegetation, leading to a positive GPP anomaly offsetting the negative tropical one. Also, the high atmospheric CO_2 growth rate in the ENSO period could be attributable partly to increased respiratory CO_2 emission. As implied by figure 2, the interplay of multiple meteorological factors (i.e. radiation, temperature, and precipitation) makes it difficult to isolate the GPP response to specific events, even an extreme one. As a result, the present models have been insufficiently constrained and calibrated in terms of responsiveness to the eruption event and similar extreme environmental variability.

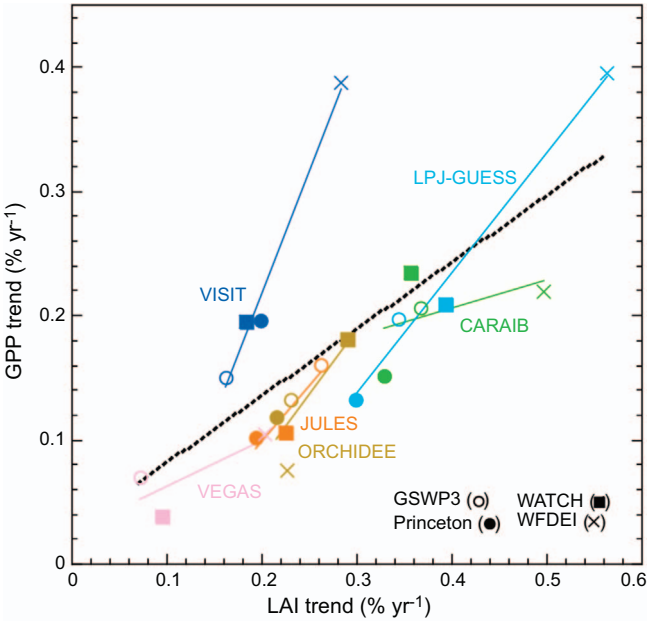

Figure 6. Relationship between the simulated trend of the leaf area index (LAI) and gross primary production (GPP).

3.6. Mechanistic findings from benchmarking

The incremental GPP trends (figure 2(*a*)) could be attributable to several mechanisms: (1) enhancement of photosynthetic capacity, (2) elongation of growing period, (3) expansion of canopy leaf area, and (4) land-use and land-cover change. As attempted by Xia *et al* (2015), factors related to leaf area (phenology and vegetation structure) and photosynthetic capacity (physiology) could be combined using an appropriate metric. The simulated GPP trend occurred heterogeneously over the land area. At a global scale, it is well correlated with the trend of mean leaf area index (LAI) trend in the different biome models and forcing datasets (figure 6). Note that several models assumed a stationary land-use and plant functional type distribution but showed a similarly positive relationship. Therefore, the incremental GPP trend was at least partly attributable to LAI expansion, which in turn, has several causes. Apparently, the CO_2 fertilization effect played an important role, but observational evidences provide inconsistent implications for the model sensitivity as noted previously (Kolby Smith *et al* 2015, Campbell *et al* 2017). We need to seek additional data and metrics to reduce the uncertainty; for example, Wenzel *et al* (2016) implied that SCA is a useful metric to constrain the simulated GPP trend.

Spatial variability in the simulated GPP trends (figure S4) has additional mechanistic implications. For each forcing dataset, positive trends occurred from tropical to boreal regions, especially in North America, Eurasia, and eastern Australia. In contrast, consistently negative trends occurred in Central America, a part of South America, and eastern Central Africa. The simulated regional GPP showed different temporal patterns in response to meteorological regimes (figure S5). For example, it is remarkable that the incremental trend continued in Asia, Africa, Europe, and North America after 2000 but almost completely disappeared in Oceania and South America. This period of the 2000s is known as the hiatus of global warming, leading to an unexpected depression of the atmospheric CO_2 growth rate probably due to suppressed ecosystem respiration (Keenan *et al* 2016, Ballantyne *et al* 2017). A regional analysis of GPP may provide a supporting evidence for the recent perturbations in the global carbon cycle, although further in-depth analyses are required.

Another implication for biome models and meteorological data is related to the solar radiation used in global simulation analyses. Although solar radiation is the ultimate driver of photosynthesis, this benchmarking study suggests that it was underrepresented in forcing data and that biome models are insufficiently constrained to capture responses to solar radiation variability (figure 2(*c*)). Solar radiation is acknowledged to be highly heterogeneous over the land surface and therefore difficult to accurately quantify at broad scales. Also, atmosphere–ecosystem interaction studies have focused more heavily on other environmental factors such as temperature, precipitation, ambient CO_2, and nutrients. However, as shown by the poor simulation results for the GPP anomaly after the Mt. Pinatubo eruption, we need more accurate solar radiation data and further refinement and constraints on modeled radiation use by terrestrial vegetation. This task is necessary not only for refining historical simulations but also for improving the reliability of future projections, including the increase of industrial aerosol emissions and deployment of solar radiation management (Mercado *et al* 2009, Caldeira *et al* 2013, Ito *et al* 2017).

4. Concluding remarks

We conducted a benchmarking of eight biome models and confirmed that these current biome models can approximately capture basic features such as the spatial distribution of productivity (i.e. capability of CO_2 fixation). Such benchmarking of model-estimated GPP has been conducted by previous model inter comparison studies (table 3), and this ISI-MIP study provided several new findings. By using multiple meteorological forcing datasets, it revealed contributions of inter-model (primary) and inter-data (secondary) variabilities. Focusing on recent decades, it was possible to assess model responses to several well-known extreme events. Importantly, the results of the biome sector could be combined with other sectors such as water and agriculture, allowing us to conduct more human-relevant analyses. Recent advancements in instruments and data-analysis studies are providing an increasing amount of data for benchmarking, allowing us to examine the validity and limitations of models in more detail. Although several benchmarking studies of biome models have been conducted, this study provided some new insights. First, this study provided results of WUE and RUE and the seasonal-cycle amplitude of GPP, allowing us to address the underlying mechanisms of the historical changes. Second, our use of multiple forcing datasets permitted us to account for a wider range of estimation uncertainty than in previous studies. The comparison emphasized the large discrepancy in solar radiation among the forcing datasets. Third, the use of flux upscaled GPP and satellite-derived SIF data provided more insights than a simple comparison between models. These findings imply that we need to improve parameterization of GPP, for example, in terms of radiation responsiveness. Although further observation and modeling studies are required, this type of benchmarking study helps to refine biome models and improve our confidence in future projections (e.g. +1.5 and +2 °C impact assessments for the Paris Agreement, conducted as the next phase of ISIMIP, i.e. ISIMIP2b) using these models.

Acknowledgments

This study was conducted as a part of the second phase of ISIMIP organized by the Potsdam Institute of Climate Impact Research (ISIMIP2a) and financed from the German Federal Ministry of Education and Research (BMBF, grant no. 01L1201A1). It used data obtained from the Deutsche Klimarechenzentrum (German Climate Computing Center) data server. P. C. acknowledges support from European Research Council Synergy grant ERC-2013-SyG-610028 IMBALANCE-P. J. C. received support from the European Commission's 7th Framework Program (EU/FP7) project. C.M. received support from the EU/FP7 under Grant Agreement 603864 (HELIX). A. I. was supported by the Environmental Research and Technology Development Fund (S-10) of the Ministry of the Environment, Japan, and a grant-in-aid (no. 26281014) from the Japan Society for the Promotion of Science.

ORCID

Akihiko Ito https://orcid.org/0000-0001-5265-0791

References

Anav A *et al* 2015 Spatio-temporal patterns of terrestrial gross primary production: a review *Rev. Geophys.* **53** 1–34

Arora V K *et al* 2013 Carbon–concentration and carbon–climate feedbacks in CMIP5 Earth system models *J. Clim.* **26** 5289–314

Baldocchi D *et al* 2001 FLUXNET: a new tool to study the temporal and spatial variability of ecosystem-scale carbon dioxide, water vapor, and energy flux densities *Bull. Am. Meteorol. Soc.* **82** 2415–34

Baldocchi D, Sturtevant C and Fluxnet-contributors 2015 Does day and night sampling reduce spurious correlation between canopy photosynthesis and ecosystem respiration? *Agric. Forest Meteorol.* **207** 117–26

Ballantyne A *et al* 2017 Accelerating net terrestrial carbon uptake during the warming hiatus due to reduced respiration *Nat. Clim. Change* **7** 148–52

Beer C *et al* 2010 Terrestrial gross carbon dioxide uptake: Global distribution and covariation with climate *Science* **329** 834–8

Betts R A, Jones C D, Knight J R, Keeling R F and Kennedy J J 2016 El Niño and a record CO_2 rise *Nat. Clim. Change* **6** 806–10

Bonan G B, Williams M, Fisher R A and Oleson K W 2014 Modeling stomatal conductance in the Earth system: linking leaf water-use efficiency and water transport along the soil–plant–atmosphere continuum *Geosci. Model Dev.* **7** 2193–222

Bondeau A *et al* 2007 Modelling the role of agriculture for the 20th century global terrestrial carbon balamce *Glob. Change Biol.* **13** 679–706

Caldeira K, Bala G and Cao L 2013 The science of geoengineering *Ann. Rev. Earth Planet. Sci.* **41** 231–56

Campbell J E *et al* 2017 Large historical growth in global terrestrial gross primary production *Nature* **544** 84–7

Chang J *et al* 2017 Benchmarking carbon fluxes of the ISIMIP2a biome models *Environ. Res. Lett.* **12** 045002

Clark D B *et al* 2011 The joint UK land environment simulator (JULES), model description—Part 2: carbon fluxes and vegetation dynamics *Geosci Model Dev.* **4** 701–22

Cox P M, Betts R A, Jones G D, Spall S A and Totterdell I J 2000 Acceleration of global warming due to carbon-cycle feedbacks in a coupled climate model *Nature* **408** 184–7

Dlugokencky E and Tans P 2014 NOAA/ESRL Global CO_2 data (www.esrl.noaa.gov/gmd/ccgg/trends/)

Dury M, Hambuckers A, Warnant P, Henrot A, Favre E, Ouberdous M and François L 2010 Responses of Europenan forest ecosystems to 21st century climate changes in interannual variability and fire intensity *Forest Biogeosci. Forestry* **4** 82–99

Frankenberg C *et al* 2011 New global observations of the terrestrial carbon cycle from GOSAT: patterns of plant fluorescence with gross primary production *Geophys. Res. Lett.* **38** L17706

Friedlingstein P *et al* 2006 Climate-carbon cycle feedback analysis: results from the C4MIP model intercomparison *J. Clim.* **19** 3337–53

Friend A D *et al* 2014 Carbon residence time dominates uncertainty in terrestrial vegetation responses to future climate and atmospheric CO_2 *Proc. Nat. Acad. Sci. USA* **111** 3280–5

Frölicher T L, Joos F, Raible C C and Sarmiento J L 2013 Atmospheric CO_2 response to volcanic eruptions: the role of ENSO, season, and variability *Glob. Biogeochem. Cycles* **27** 239–51

Genty B, Briantais J-M and Baker N R 1989 The relationship between the quantum yield of photosynthetic electron transport and quenching of chlorophyll fluorescence *Biochim. Biophys. Acta* **990** 87–92

Graven H D *et al* 2013 Enhanced seasonal exchange of CO_2 by northern ecosystems since 1960 *Science* **341** 1085–9

Gu L *et al* 2002 Advantages of diffuse radiation for terrestrial ecosystem productivity *J. Geophys. Res.* **107** 4050

Guanter L *et al* 2014 Global and time-resolved monitoring of crop photosynthesis with chlorophyll fluorescence *Proc. Nat. Acad. Sci. USA* **111** E1327–33

Ito A *et al* 2017 Solar radiation management and ecosystem functional responses *Clim. Change* **142** 53–66

Ito A and Inatomi M 2012 Water-use efficiency of the terrestrial biosphere: a model analysis on interactions between the global carbon and water cycles *J. Hydrometeorol.* **13** 681–94

Ito A *et al* 2016 Decadal trends in the seasonal-cycle amplitude of terrestrial CO_2 exchange resulting from the ensemble of terrestrial biosphere models *Tellus* B **68** 28968

Joiner J *et al* 2013 Global monitoring of terrestrial chlorophyll fluorescence from moderate-spectral-resolution near-infrared satellite measurements: methodology, simulations, and application to GOME-2 *Atmos. Meas. Technol.* **6** 2803–23

Jung M, Reichstein M and Bondeau A 2009 Towards global empirical upscaling of FLUXNET eddy covariance observations: validation of a model tree ensemble approach using a biosphere model *Biogeosciences* **6** 2001–13

Jung M *et al* 2017 Compensatory water effects link yearly global land CO_2 sink changes to temperature *Nature* **541** 516–20

Kanniah K D, Beringer J and Hutley L 2013 Exploring the link between clouds, radiation, and canopy productivity of tropical savannas *Agric. Forest Meteorol.* **182/183** 304–13

Keeling C D, Whorf T P, Wahlen M and van der Plicht J 1995 Interannual extremes in the rate of rise of atmospheric carbon dioxide since 1980 *Nature* **375** 666–70

Keenan T F *et al* 2013 Increase in forest water-use efficiency as atmospheric carbon dioxide concentration rise *Nature* **499** 324–7

Keenan T F *et al* 2016 Recent pause in the growth rate of atmospheric CO_2 due to enhanced terrestrial carbon uptake *Nat. Commun.* **7** 13428

Kelley D I *et al* 2013 A comprehencive benchmarking system for evaluating global vegetation models *Biogeosciences* **10** 3313–40

Kiehl J T and Trenberth K E 1997 Earth's annual global mean energy budget *Bull. Am. Meteorol. Soc.* **78** 197–208

Koffi E N, Rayner P J, Scholze M, Chevallier F and Kaminski T 2013 Quantifying the constraint of biospheric process parameters by CO_2 concentration and flux measurement networks through a carbon cycle data assimilation system *Atmos. Chem. Phys.* **13** 10555–72

Kolby Smith W *et al* 2015 Large divergence of satellite and Earth system model estimates of global terrestrial CO_2 fertilization *Nat. Clim. Change* **6** 306–10

Krinner G *et al* 2005 A dynamic global vegetation model for studies of the coupled atmosphere-biosphere system *Glob. Biogeochem. Cycles* **19** GB1015

Kuppel S *et al* 2014 Model-data fusion across ecosystems: from multisite optimizations to global simulations *Geosci. Model Dev.* **7** 2581–97

Le Quéré C *et al* 2015 Global carbon budget 2015 *Earth Sys. Sci. Data* **7** 349–396

Lucht W *et al* 2002 Climatic control of the high-latitude vegetation greening trend and Pinatubo effect *Science* **296** 1687–9

Luo Y *et al* 2012 A framework for benchmarking land models *Biogeosciences* **9** 3857–74

Ma J, Yan X, Dong W and Chou J 2015 Gross primary production of global forest ecosystems has been overestimated *Sci. Rep.* **5** 21378

McCormick M P, Thomason L W and Trepte C R 1995 Atmospheric effects of the Mt Pinatubo eruption *Nature* **373** 399–404

McCree K J 1972 Test of current definitions of photosynthetically active radiation against leaf photosynthesis data *Agric. Meteorol.* **10** 443–53

Medlyn B E *et al* 2001 Stomatal conductance of forest species after long-term exposure to elevated CO_2 concentration: a synthesis *New Phytol.* **149** 247–64

Meinshausen M *et al* 2011 The RCP greenhouse gas concentrations and their extensions from 1765 to 2300 *Clim. Change* **109** 213–241

Mercado L M *et al* 2009 Impact of changes in diffuse radiation on the global land carbon sink *Nature* **458** 1014–7

Nishina K *et al* 2015 Decomposing uncertainties in the future terrestrial carbon budget associated with emission scenario, climate projection, and ecosystem simulation using the ISI-MIP result *Earth Sys. Dyn.* **6** 435–45

Porcar-Castell A, Tyystjärvi E, Atherton J, van der Tol C, Flexas J, Pfündel E E, Moreno J, Frankenberg C and Berry J A 2014 Linking chlorophyll a fluorescence to photosynthesis for remote sensing applications: mechanisms and challenges *J. Exp. Bot.* **65** 4065–95

R Core Team 2017 R: A language and environment for statistical computing *R Foundation for Statistical Computing* (Vienna: Austria)

Reichstein M *et al* 2005 On the separation of net ecosystem exchange into assimilation and ecosystem respiration: review and improved algorithm *Glob. Change Biol.* **11** 1424–39

Roderick M L, Farquhar G D, Berry S L and Noble I R 2001 On the direct effect of clouds and atmospheric particles on the productivity and structure of vegetation *Oecologia* **129** 21–30

Rosenzweig C *et al* 2017 Assessing inter-sectoral climate change risks: the role of ISIMIP *Environ. Res. Lett.* **12** 010301

Ruimy A, Kergoat L, Bondeau A, Potsdam N P P and Model Intercomparison participants 1999 Comparing global NPP models of terrestrial net primary productivity (NPP): analysis of differences in light absorption and light-use efficiency *Glob. Change Biol.* **5** 56–64

Ryu Y *et al* 2011 Integration of MODIS land and atmosphere products with a coupled-process model to estimate gross primary productivity and evapotranspiration from 1 km to global scales *Glob. Biogeochem. Cycles* **25** GB4017

Schimel D, Stephens B B and Fisher J B 2015 Effect of increasing CO_2 on the terrestrial carbon cycle *Proc. Nat. Acad. Sci. USA* **112** 436–41

Schwalm C *et al* 2015 Toward 'optimal' integration of terrestrial biosphere models *Geophys. Res. Lett.* **42** 1–11

Sheffield J, Goteti G and Wood E F 2006 Development of a 50-year high-resolution global dataset of meteorological forcings for land surface modeling *J. Clim.* **19** 3088–111

Sitch S *et al* 2015 Recent trends and drivers of regional sources and sinks of carbon dioxide *Biogeosciences* **12** 653–679

Smith B, Prentice I C and Sykes M T 2001 Representation of vegetation dynamics in the modeling of terrestrial ecosystems: comparing two contrasting approaches within European climate space *Glob. Ecol. Biogeogr.* **10** 621–37

Tian H *et al* 2011 China's terrestrial carbon balance: Contributions from multiple global change factors *Glob. Biogeochem. Cycles* **25** GB1007

Weedon G P *et al* 2014 The WFDEI meteorological forcing data set: watch forcing data methodology applied to era-interim reanalysis data *Water Resour. Res.* **50** 7505–14

Wehr R *et al* 2016 Seasonality of temperate forest photosynthesis and daytime respiration *Nature* **534** 680–3

Welp L R *et al* 2011 Interannual variability in the oxygen isotopes of atmospheric CO_2 driven by El Niño *Nature* **477** 579–82

Wenzel S, Cox P M, Eyring V and Friedlingstein P 2016 Projected land photosynthesis constrained by changes in the seasonal cycle of atmospheric CO_2 *Nature* **538** 499–501

Whittaker R H and Likens G E 1973 Primary production: the biosphere and man *Human Ecol.* **1** 357–69

Wild M 2012 Enlightening global dimming and brighening *Bull. Am. Meteorol. Soc.* **93** 27–37

Xia J *et al* 2015 Joint control of terrestrial gross primary productivity by plant phenology and physiology *Proc. Nat. Acad. Sci. USA* **112** 2788–93

Xue B-L, Guo Q, Otto A, Xiao J, Tao S and Li L 2015 Global patterns, trends, and drivers of water use efficiency from 2000 to 2013 *Ecosphere* **6** 174

Yan H *et al* 2015 Improved global simulations of gross primary product based on a new definition of water stress and a separate treatment of C_3 and C_4 plants *Ecol. Model.* **297** 42–59

Yebra M, van Dijk A I J M, Leuning R and Guerschman J P 2015 Global vegetation gross primary production estimation using satellite-derived light-use efficiency and canopy conductance *Remote Sens. Environ.* **163** 206–16

Zaehle S *et al* 2014 Evaluation of 11 terrestrial carbon–nitrogen cycle models against observations from two temperate free-air CO_2 enrichment studies *New Phytol.* **202** 803–22

Zeng N, Mariotti A and Wetzel P 2005 Terrestrial mechanisms of interannual CO_2 variability *Glob. Biogeochem. Cycles* **19** GB1016

Zhang Y *et al* 2016a Development of a coupled carbon and water model for estimating global gross primary productivity and evapotranspiration based on eddy flux and remote sensing data *Agric. Forest Meteorol.* **223** 116–31

Zhang Y *et al* 2016b Consistency between sun-induced chlorophyll fluorescence and gross primary production of vegetation in North America *Remote Sens. Environ.* **183** 154–69

Zhang Y *et al* 2016c Precipitation and carbon-water coupling jointly control the interannual variability of global land gross primary production *Sci. Rep.* **6** 39748

Zhao F and Zeng N 2014 Continued increase in atmospheric CO_2 seasonal amplitude in the 21st century projectes by the CMIP5 Earth system models *Earth Sys. Dyn.* **5** 423–39

Zhao M, Heinsch F A, Nemani R and Running S W 2005 Improvements of the MODIS terrestrial gross and net primary production global data set *Remote Sens. Environ.* **95** 164–76

Zhu Z *et al* 2016 Greening of the Earth and its drivers *Nat. Clim. Change* **6** 791–5